Registration of Histologic Colour Images of Different Staining

Ulf-Dietrich Braumann[1], Jens Einenkel[2], Lars-Christian Horn[3], Jens-Peer Kuska[1], Markus Löffler[1], Nico Scherf[1] and Nicolas Wentzensen[4]

[1]Interdisziplinäres Zentrum für Bioinformatik, Universität Leipzig, 04107 Leipzig
[2]Universitätsfrauenklinik Leipzig, 04103 Leipzig
[3]Institut für Pathologie, Universität Leipzig, 04103 Leipzig
[4]Pathologisches Institut, Universität Heidelberg, 69120 Heidelberg
Email: braumann@izbi.uni-leipzig.de

Abstract. We have focused our interest on the registration of brightfield transmitted light microscopy images with respect to different histological stainings. For this kind of registration problem we have developed a new segmentation procedure. Based on the obtained consistent segmentations, a nonlinear registration transformation is computed. The applied registration procedure uses a curvature-based nonlinear partial differential equation in order to find the appropriate mapping between the images. Finally, we present an example for the registration of images of two consecutive histological sections from a uterine cervix specimen, whereas one section stained with $p16^{INK4a}$ was mapped onto another with H&E staining.

1 Introduction

The use of diverse stainings of consecutive tissue sections can provide a valuable amount of additional information about the structure and position of different types of tissues. Especially the usage of different immunohistochemical stainings may provide new insights into the interaction of cancer, inflammation and healthy cells in the human body. Multiple- or even double-staining techniques using different immunohistochemical stains applied on *one and the same* section is difficult due to the interaction of the staining agents, and in many cases is not feasible. One solution for that problem might be the usage of consecutive sections, while the application of different staining protocols is accomplished on separate slices.

What basically makes the registration of images of such sections difficult is the partial loss of spatial correspondences between the two sections. The reasons for the deformation between consecutive sections are not only some differences concerning the mechanical stress applied during the preparation, especially while sectioning. The aggressive chemical substances used for the staining usually cause some individual, non-uniform shrinkage of the different tissue types which may be comprised within a certain section. To reconstruct the spatial correspondences between the individual sections the usage of a basically nonlinear registration

procedure is required. However, the registration of differently stained images is not at all straightforward, due to the fact that different stainings may have totally different distributions both in colour as well in position space. So the direct usage of the colour images for the registration process is not possible. This is why we need to accomplish a segmentation step prior to the actual registration which, however, requires the utmost possible consistency referring to the various applied stainings. We consider this intermediate step essential in order to obtain the optimum accuracy for the respective registration transformation.

As the segmentation leads to label images, the registration procedure itself still remains based on scalar image data. Depending on the segmentation quality, the registration will restore the correspondences between the tissue boundaries, however some possible correspondence on the level of individual cells is lost. One important restriction of the developed method is the requirement that important (large area) tissue types must be distinguishable in *all* staining variants.

2 Segmentation

The segmentation plays the central role in the registration of the slices with unequal colours. We focus our interest on the statistical description of the distribution of pixel properties in a d-dimensional feature space. Every staining has an individual distribution in the applied colour space. We operate in the RGB space, but other colour spaces may be used as well. The identification of different tissue types does not only include pixel differences within the colour space. The statistical properties of a pixel's neighbourhood may also be important[1, 2, 3]. To include these properties into the segmentation, we construct a d-dimensional vector from selected statistical properties of the pixel, see Fig. 1. The neighbourhood is included in the segmentation vector using properties like the colour mean value and by the construction of successive smoothed images (the level index l in Fig. 1). Frequency properties of the respective pixel are included via sampling along an Archimedian spiral, starting at the pixel and analyzing the frequency distribution of the one-dimensional Fourier transform.

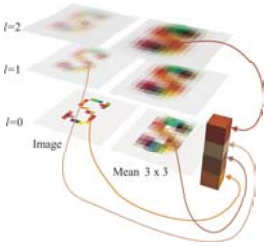

Fig. 1. Construction of the segmentation vector from colour and mean and some smoothing levels. In this example the segmentation vector is constructed from the colour of the image and the Gaussian smoothed image, than the mean value of the unsmoothed and the two times smoothed image, giving a 3×4 dimensional segmentation vector.

The segmentation vectors $\mathbf{y}_i$ are used to estimate the distribution

$$P(\mathbf{y}) = \sum_{k=1}^{K} \alpha_k \, p(\mathbf{y}|\mu_\mathbf{k}, \Sigma_k) \tag{1}$$

as a linear combination of normal distributions

$$p(\mathbf{y}|\mu, \Sigma) = \frac{(2\,\pi)^{-d/2}}{\sqrt{\det \Sigma}} \exp\left(-\frac{1}{2}(\mathbf{y}-\mu)^T \cdot \Sigma^{-1} \cdot (\mathbf{y}-\mu)\right). \tag{2}$$

The estimation of the paramters μ_k, Σ_k and α_k is done using the expectation maximization algorithm [4, 5]. Using the estimated distribution $P(\mathbf{y})$ we assign every pixel in the image a class number

$$\arg\max_k \frac{\alpha_k\, p(\mathbf{x}|\mu_\mathbf{k}, \Sigma_k)}{\sum_{k=1}^{K} \alpha_k\, p(\mathbf{x}|\mu_\mathbf{i}, \Sigma_i)} \tag{3}$$

to obtain the image segmentation.

For the two slices with different staining we obtain two segmented images S and S', whereas the class labels assigned by the algorithm must be made consistent between the two segmentations. This means, that the labels in one of the segmentations, say S', must be exchanged to match the same regions as in the image S. The segmentation S' may have more classes K' than the segmentation S with K classes. This could occur, for instance, when the second staining marks vessels that cannot be identified in the first staining. In such case the class labels must be merged to describe the same region in both segmentations. Merging of two or more classes is also necessary, when a good approximation of the density distribution requires more than a single normal distribution to describe the segmentation vectors of a certain tissue type in one of the two colour images.

3 Registration

From the segmentation we get two images with scalar class label information. These two scalar images are used to compute the displacement field $\mathbf{u}(\mathbf{x})$ for the registration. The computation of the displacement field $\mathbf{u}$ base on the partial differential equation

$$\alpha\, \Delta^2 \mathbf{u} - \mathbf{f}(\mathbf{x}, \mathbf{u}) = 0 \tag{4}$$

with

$$\mathbf{f}(\mathbf{x}, \mathbf{u}) = [S'(\mathbf{x}) - S(\mathbf{x} - \mathbf{u}(\mathbf{x}))]\, \nabla S(\mathbf{x} - \mathbf{u}(\mathbf{x})) \tag{5}$$

This equation was introduced in [6] and recently studied in [7], wherein Δ denotes the two-dimensional Laplace operator. To allow a smooth convergence for the solution, we introduce an artificial time t and solve the equation

$$\frac{\partial \mathbf{u}}{\partial t}(\mathbf{x}, t) + \alpha\, \Delta^2 \mathbf{u}(\mathbf{x}, t) = \mathbf{f}(\mathbf{x}, \mathbf{u}(\mathbf{x}, t)) \tag{6}$$

The time discretisation is done by an implicit midpoint rule, and the dependence on the position coordinate $\mathbf{x}$ in the finite difference approximation of Δ^2 is resolved using a discrete cos-transform. A detailed description about the solution procedure and the used finite difference approximations can be found in [8]. Finally, when the displacement field for the registration is found, the original colour image is transformed according to this transformation to obtain the registered version of the original data.

Fig. 2. Label exchange and label merging (black circle) to obtain a consistent segmentation for a H&E and $p16^{INK4a}$ stained image pair.

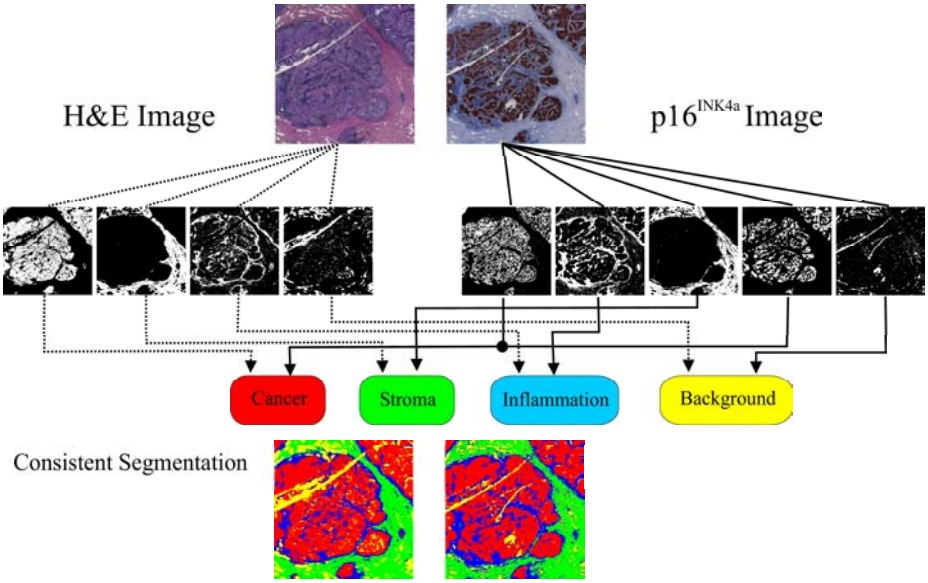

4 Example

As an example for the process outlined above, we consider two images with H&E and $p16^{INK4a}$ staining, respectively, that should be registered. The tissue types that appear in both images are cancer, inflammation, healthy stroma and additionally the background. This suggests a total of four classes for the segmentation. For the segmentation of the H&E image we use two smoothing levels and choose the colour, the mean value in a 7×7 neighbourhood of level $l = 0$, and the slope of the frequency distribution from the first smoothing level. The $p16^{INK4a}$ image is segmented using the colour of level $l = 0$ and the colour from the first smoothing level. For the $p16^{INK4a}$ image we need an additional normal distribution to describe the colour of the cancer region. We end up with four classes for the H&E image and five classes for the $p16^{INK4a}$ staining. The colour labels of the $p16^{INK4a}$ segmentation were re-sorted, and the two classes for the cancer region were merged (see Fig. 2 for the summary of the operations). The consistent segmentations obtained by these operations were used to compute the displacement field and were further applied to the original $p16^{INK4a}$ stained image. The result of this operation can be seen in the left part of Fig. 3. To underline the quality of the image registration obtained by the proposed method we show the result for a alternating sequence of H&E and $p16^{INK4a}$ stained images. The consistent segmentation of every slice were registered on the consistent segmentation of its predecessor. The right part of Fig. 3 shows the result of this procedure.

Fig. 3. Left: Registration field (red lines) obtained by the registration of the segmentations of a $p16^{INK4a}$ image (green channel) onto a H&E stained image (red channel) with the transformed segmentation (blue channel). Middle & right: Illustrative assessment of the obtained reconstruction for an alternating H&E/$p16^{INK4a}$ stained serial section. The oblique plane in the middle image depicts how the virtual cutting plane was basically placed for the virtual section given on the right image.

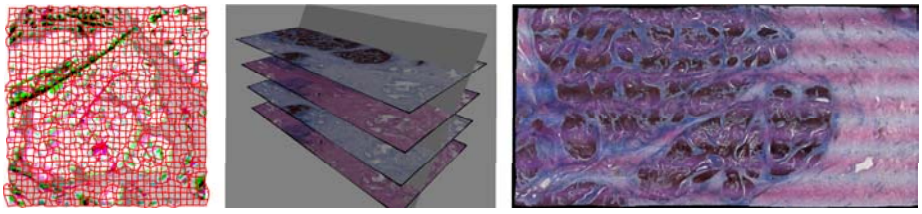

5 Conclusions and future work

We have shown a method for the registration of microscopic sections with different stainings on the base of the consistent segmentation of the respective images. The method was successfully applied onto an alternating sequence of H&E/$p16^{INK4a}$ stained images. Our work continues with the application of the newly developed method for other stainings and the registration of serial sections with more than just two different stainings.

References

1. Manjunath BS, Ohm JR, Vasudevan VV, Yamada A. Color and Texture Descriptors. IEEE Transactions on Circuits and Systems for Video Technology 2001;11(6):703–715.
2. Lucchese L, Mitra SK. Color Image Segmentation: A State-of-the-Art Survey. Proceeding of the Indian National Science Academy A (Physical Sciences) 2001;67(2):207–221.
3. Manjunath BS, Ma WY. Texture Features for Browsing and Retrival of Image Data. IEEE Transactions on Pattern Analysis and Machine Intelligence 1996;18(10):837–842.
4. Moon TK. The Expectation-Maximization Algorithm. IEEE Signal Processing Magazine 1996;p. 47–60.
5. Pernkopf F, Bouchaffra D. Genetic-Based EM Algorithm for Learning Gaussian Mixture Models. IEEE Transactions on Pattern Analysis and Machine Intelligence 2005;27(8):1344–1348.
6. Amit Y. A Nonlinear Variational Problem for Image Matching. SIAM Journal on Scientific Computing 1994;15(1):207–224.
7. Fischer B, Modersitzki J. Curvature Based Image Registration. Journal of Mathematical Imaging and Vision 2003;18:81–85.
8. Braumann UD, Kuska JP, Einenkel J, Horn LC, Löffler M, Höckel M. Three-Dimensional Reconstruction and Quantification of Cervical Carcinoma Invasion Fronts from Histological Serial Sections. IEEE Transactions on Medical Imaging 2005;24(10):1286–1307.